DUAL LABELING OF SYNGENEIC TUMOR CELLS FOR *IN VIVO* AND *IN VITRO* LOCALIZATION

A PROJECT
SUBMITTED TO THE FACULTY OF THE GRADUATE SCHOOL
OF THE UNIVERSITY OF MINNESOTA
BY

Edward Anthony Zamora

IN PARTIAL FULFILLMENT OF THE REQUIREMENTS
FOR THE DEGREE OF
MASTER OF SCIENCE

JAIME MODIANO, V.M.D, Ph.D., Advisor

August, 2012

Acknowledgements

I would like to thank my committee members first and foremost: Dr. Jaime Modiano, Dr. Scott Dehm, and Dr. Chris Pennell. I would also like to thank Dr. Jaime Modiano for mentoring me and allowing me the opportunity to conduct research in his laboratory. I would also like to especially thank Dr. John Ohlfest for having the courage to take on his first stray into his laboratory. Without it, I would not have had the opportunity to break away from my former career and nurture my interest in bench research.

Dedication

I would like to dedicate this thesis to my wonderful wife Julie and my beautiful daughter Lila. I am sorry that this endeavor took so long. “You are my ladies” and I never want to change that.

Abstract

Animal models in cancer research have been critical to much of our understanding of tumor biology. However, while early models have advanced the field, improvements need to be made if we are to realize the ultimate goal of translational relevance. In this research, we sought to address the difficulties of *in vivo* and *in vitro* tumor cell tracking and localization by using two established models, B16 melanoma and Lewis lung carcinoma. To this end, cells were stably transfected with a dual reporter vector containing green fluorescent protein (*GFP*) and firefly luciferase (*fLuc*) genes and clonal isolates were compared with parental lines. In at least one instance, the monoclonal tumor model, LLC_GL:HI2 was shown to retain tumorigenic potential while also retaining expression of the reporter genes *in vivo* and *in vitro*.

Table of Contents

Table of Contents

INTRODUCTION

The term ‘cancer’ encompasses many diseases. As defined by Hanahan and Weinberg in the now seminal report “The Hallmarks of Cancer” [1] there are multiple common characteristics that are relevant to cancer. Since that initial report, Hanahan and Weinberg expanded the list to include ten distinct variables to define cancer [2]. Importantly, this demonstrates that ‘cancer’ as a whole is a complex set of diseases within which are dozens, if not hundreds, of categories. In this given context it is not difficult to appreciate how closely related cancers have unique properties, and thus present unique challenges to understand and properly treat them.

One of the many challenges to the study of cancer is the model within which science is confined. As it is unreasonable, impractical, and unethical to perform certain types of studies in humans, multiple model types have been created. These are categorized primarily into two universal approaches: *in vitro* tissue culture systems and *in vivo* animal based systems. As each have their respective advantages and disadvantages, both are frequently used to provide collaborative and complimentary evidence.

Cell lines are typically created from animal and human tumors, and therefore represent an easily modified *in vitro* source for studying health and disease. Much research has been conducted solely based upon established or “immortal” cell lines as they proliferate indefinitely given proper growth conditions. This considerable advantage allows for tremendous expansion at rapid rates. Tissue culture models are responsible for the earliest progress in

cancer research, allowing for controlled experimental conditions and enabling fundamental studies into gross morphology, assessment of proliferation, differentiation, transcription, translation, and other molecular mechanisms. They also allow for the manipulation of various protein or molecular targets through the use of reagents and with relatively low cost, firmly securing their place within cancer research [3].

In addition to the extracellular modifications which are frequently employed in culture models, it is also possible to apply direct genetic modification techniques such as viral transduction or plasmid transfection to alter cells on a large scale. These tools have also provided tremendous insight into normal intracellular behaviors within a cell line. For instance, proteins fused to fluorescent markers have repeatedly allowed the visualization and monitoring of *in vitro* cultures [4-6]. This has facilitated tracking and localization of proteins in real time under a multitude of *in vitro* and *in vivo* conditions.

However, cancer research that is restricted to the use of cell cultures has major limitations. For example, cross contamination of cultures with other cell lines is a major concern [7, 8]. As cell lines have acquired the ability to proliferate indefinitely, they are utilized during extended periods of time and passaging, continuously risking exposure and therefore potential contamination from other cells. It has been suggested that in many cases, cell lines have been overtaken by faster growing contaminant cells, such as HeLa, and thus made the data difficult to interpret [9]. These factors and others mentioned above make it vital to validating cell lines on a consistent and ongoing basis

using techniques such as short tandem repeat STR profiling to establish genetic fingerprinting, fluorescent in situ hybridization (FISH) to detect and localize specific sequences to chromosomes, and mycoplasma testing for potential sources of cell alterations [8].

Even assuming that contamination is not present, culture-based research is also subject to some limitations that can make data difficult to interpret. For instance, cell lines kept in culture must overcome cellular senescence and crisis, and during this process they can develop numerical and structural chromosomal abnormalities. Possibly reflecting such genetic changes, tumor lines that have been removed from contextual tissues often foster changes in their normal biology [10]. Furthermore, as our understanding of tumor-specific stromal biology has progressed, it has become clear that other limitations exist. Specifically, examples include tissue-specific oxygen variance, loss of stromal–based exchange of cytokines, loss of vascular architecture and loss of inflammatory signaling [11]. Thus it has become necessary to address these issues and approach the study of cancer from multiple perspectives and alternative models.

In conjunction with cell cultures, animal models have been utilized to study cancer for over a century. One model which is commonly exploited is the mouse model (*Mus musculus*), which has multiple benefits in the laboratory setting. First, as it is a mammal, it has many parallels to human molecular and physiological mechanisms. Though its size is greatly reduced, such similarities as disease progression can still be studied in some detail. It also has a short 3-

year life span which makes timed trials more efficacious [11]. Furthermore, the recent completion of the mouse's genomic sequencing has demonstrated the mouse's genome to have considerable similarities to the human genome. As determined by both evidence-based analyses and *de novo* gene predictions, the proportion of mouse genes with single orthologues in the human genome approximates to 80% [12].

In addition to the many advantages, some drawbacks must be recognized when using murine models. Foremost amongst these is the ability of the mouse to successfully emulate the nature of many human diseases. While there are strains of mice in which cancer spontaneously develops or can be induced, such models are restricted to a subset of disease and pre-suppose that 'endogenous' tumors have similar natural histories as they do in human patients.

To try and address some of these issues, models using transplantations within genetically modified mice were developed. In particular, xenografts in immune-compromised athymic nude mice offer the primary benefit of inoculating human patient-derived specimens into the murine model for study [13, 14]. While these mice retain active natural killer (NK) cells and innate inflammation, the adaptive T-lymphocyte-related immune niche is lacking and therefore these models are not applicable in many immune-based cancer studies [15]. Some have gone so far as to suggest that the limitations in immune compromised mice are enough to reclassify these models as 'animal

cultures' since they are considered a compromise between tissue culture and mouse models [11].

As technological enhancements have expanded; the ability to create more relevant research platforms has evolved to include genetically engineered mouse models (GEMMs). While there are a few methods by which GEMMs are produced, including pronuclear injection and proviral transduction in embryonic cells [16, 17], the techniques allow various modifications including gene knockouts, conditional mutations, and even inducible control of transgene expression [18]. Regardless of the methods, the results offer better drug target validations and enable a more thorough understanding of toxicity and resistance [19]. Over all, gene manipulation enables the creation of any number of unique GEMMs that more accurately recapitulate the corresponding human disease. However, such models also require years of backcrossing backgrounds for rigorous comparison of different mutations, which is time consuming and relatively cost prohibitive.

A significant barrier to studying cancer within animal models is the lack of *in vivo* tracking and visualization. Unlike cell cultures, once inoculated, cancer cells may migrate away from the initial site of injection, expand, disappear, or otherwise become difficult to precisely monitor *in vivo*. Straightforward solutions to these problems include imprecise caliper measurements for subcutaneous tumors and monitoring fluorescently labeled transplanted cells through the skin or shaved fur. However, these methods are restricted by detection limits and thus quantification of tumor burden normally requires

animal sacrifice. This is particularly cumbersome and resource intensive during longitudinal studies, where to gain statistical power, experiments require large numbers of animals that must be sacrificed for each time point.

Alternatively, monitoring of bioluminescence using an *in vivo* imaging system (IVIS) has become a powerful tool in cancer research. This system is founded on the basis of substrate activation as an indirect readout for cells expressing specific luciferase enzymes. Specifically, an ATP-dependent oxidation of a luciferin salt by the firefly luciferase enzyme produces a photon emission signal which can be detected using a sensitive imaging system. Bioanalytical applications include the investigation of protein–protein interactions, gene expression and gene regulation [20]. Due to the inherent enzymatic requirements to create the signals, these systems only function within live cells. Thus they are an accurate surrogate for cell quantification *in vivo*, but when tissues are resected and fixed for analysis, tracking must be performed using alternative modalities.

Within this context of creating more relevant models by which cancer can be investigated, we hypothesized that we could develop a model that bridges some of the gaps in knowledge unaddressed by other systems. Our goals were to combine two previously defined approaches to cancer modeling. Specifically, we hypothesized we could perform *in vitro* labeling of established tumor cell lines, B16 melanoma and Lewis Lung Carcinoma (LLC), with stable integration of dual reporter vectors, encoding green fluorescent protein (*GFP*) and firefly luciferase (*fLuc*). We further hypothesize we could leverage these

novel cell lines via transplantation within a syngeneic, C57BL/6 mouse model to address the difficulties of *in vivo* and *in vitro* post mortem tumor cell tracking and localization.

While there are studies which have created similar reporter models, most are based on transient expression, express only one reporter, or utilize viral based delivery vehicles. This approach uses a combination of electroporation delivery and the plasmid-based Sleeping Beauty (SB) transposition system for introducing the dual reporter expression cassette into the parental tumor cell lines [21]. The SB system is composed of a transposase enzyme, SB100X, and dual-reporter plasmid transposons containing a *GFP* and *fLuc* cargo genes [22]. The two respective reporter vectors used in labeling LLCs and B16s, though unique, are similar in properties and size and thus comparable in potential integration and function. Moreover, as the transposon system is non-viral, it also offers greater simplicity and reduced potential toxicity over viral transposition methods.

Furthermore, the parental cell lines we selected reflect the need for uniquely suited, immune competent models to address immunological cancer studies. As the two cell lines, B16 and LLC, are derived from spontaneous C57BL/6 murine tumors, we may target their transplantation into genetically identical, immunoreplete mice with minimal concern for rejection. Though it should be cautioned that expression levels of these proteins have been shown to illicit immune responses [23, 24], and therefore may affect such

immunological studies, this model attempts to avoid controversy regarding immune-deficient models.

METHODS AND MATERIALS

Cell lines

The B16 murine melanoma cell line was obtained from the American Type Culture Collection (Manassas, VA) and maintained in Dulbecco's modified Eagle's medium (DMEM), containing sodium pyruvate and L-glutamine, with 10% (v/v) fetal calf serum (FCS), and 1% (v/v) Primocin (Invivogen, San Diego, CA). The LLC cell line was obtained from ATCC (Manassas, VA) and was maintained in the same modified DMEM with 10% (v/v) FCS, and 1% (v/v) Primocin. Following successful transfection, stable cell lines expressing green fluorescence protein (GFP) and firefly luciferase (fLuc) were referred to as B16_GL and LLC_GL respectively. For *in vitro* experimental controls, mesenchymal stem cells (MSCs) were obtained from Invitrogen (Life Technologies, Carlsbad, CA) and maintained in D-MEM/F-12 with 10% FCS (v/v), and 1% Primocin (v/v). MSCs were labeled using a plasmid vector containing TD tomato reporter gene (MSCs-tDt).

Lonza Nucleofection

Unless otherwise specified, all cell culture and electroporation was conducted under sterile conditions under biosafety containment hoods. Preparation of Nucleofector Solution V (Lonza, Walkersville, MD) was conducted according to the vendor instructions. Six well plates were prepared in advance as specified; wells were filled with 1mL of complete culture medium then warmed to 37°C. Cells were harvested from tissue culture flasks using trypsin-EDTA (0.25% trypsin, 1 mM EDTA) (Life Technologies, Carlsbad, CA) for

dissociation. Cells were resuspended in complete culture medium to neutralize the trypsin, counted and pelleted. Media was removed and pellets were resuspended in room temperature Cell Line Nucleofector Solution V to a final density of 1-2 x 10^6 cells/100µL. Immediately following resuspension, plasmid vector DNA was added, and the mixture was transferred to a Nucleocuvette (gap width: 0.2 cm). A GFP encoded plasmid, pMax-GFP, was provided by the vendor as a positive control vector. Following DNA addition, the cuvette was subsequently inserted into the cuvette holder in the programmed Nucleofector device, and the programming, P-020 and CM-150 for LLCs and B16s respectively, was initiated. Following the completion of the respective electroporation programs, the cells were immediately pipetted into the pre-heated six-well plates and incubated in a humidified 37°C, 5% CO_2 incubator. Plates were monitored, imaged and passaged into larger culture flasks and subjected to antibiotic selection.

Plasmid Production

The vector plasmid 1 (PGK-Zeo:GFP_CLP luc) was a generous gift of Dan Kaufman (University of Minnesota). This plasmid was created to allow the use of phosphoglycerate kinase (PGK) promoter to drive the expression of the *GFP* reporter and Zeocin™ (Zeo, Life Technologies, Carlsbad, CA) antibiotic resistance genes respectively. A second reporter, *fLuc*, is driven by an independent constitutive promoter. The vector plasmid 2 (pKT2PGK-Bsd:GFP_CLP-Luc) (Figure 1) was made possible through the generous gift of

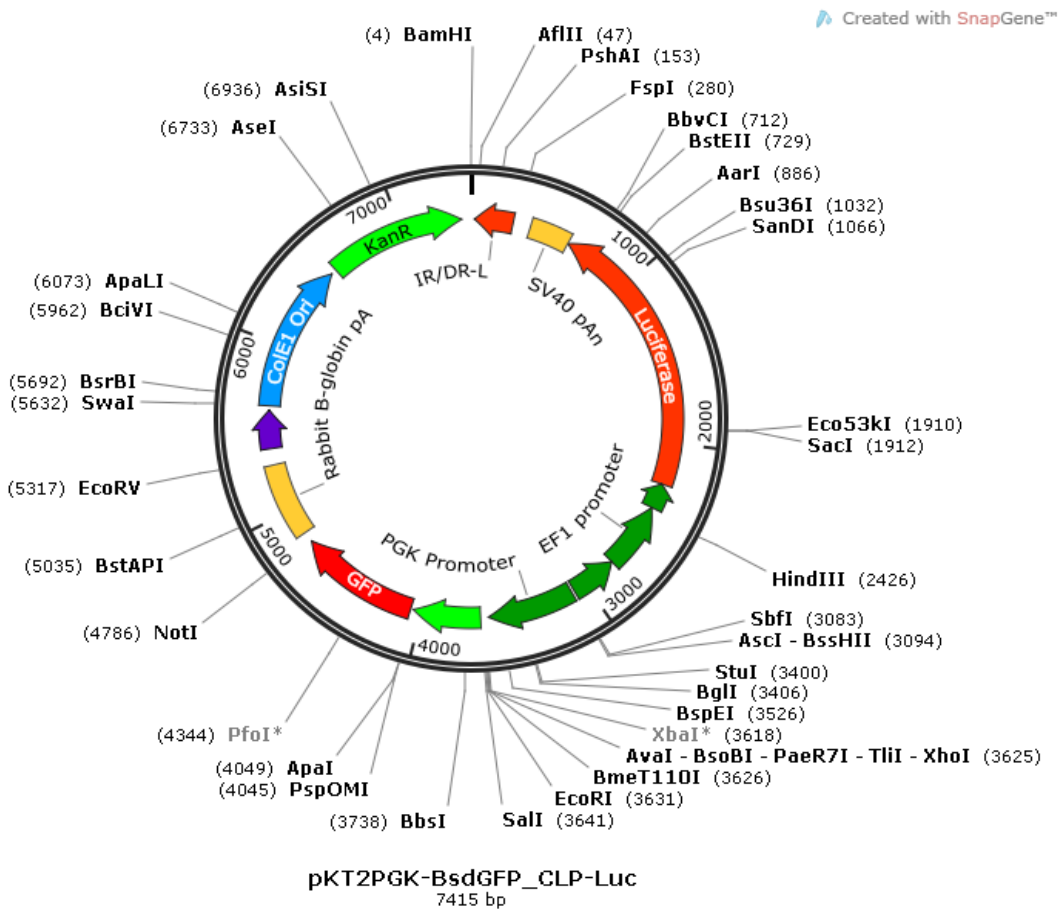

Figure 1. Plasmid 2, pKT2PGK-Bsd:GFP_CLP-Luc.

John Ohlfest, Ph.D. This plasmid was created to use a PGK promoter for the expression of the GFP and blasticidin antibiotic resistance genes. Expression of a second reporter gene, *fLuc*, is driven by the mouse cytomegalovirus (mCMV) enhancer and elongation factor-1(EF1) promoter. A schematic map ofthis second plasmid is shown in Figure 1. The total size of this plasmid is approximately 7.4 kb. Plasmids were purified using EndoFree plasmid Maxi preps (Life Technologies, Carlsbad, CA).

Flow Cyotmetry/ sorting

Transfected tumor cells were enriched using fluorescence activated cell sorting (FACS) on a FACSAria I system (BD Biosciences, San Jose, CA) using a 20mW 488 nm laser source, a 530/30 bandpass detection filter and a 100um nozzle aperture. The GFP positive cells were sorted into 2 populations, GFP^{HI} and GFP^{LO}, based on mean fluorescent intensity (MFI). The GFP^{HI} population was selected from those cells closest to the MFI peak of expression based on assumptions that higher levels of expression could be correlated to either high quantity of insertions or result in adverse effects on cellular biology [25]. The GFP^{LO} selection was based on a reduced fluorescent intensity respective of the GFP^{HI} gating. Each population was subjected to a post-sort verification of intensity and mutual exclusion of the other.

MTS Assay

Cell viability was determined using the colorimetric Cell Titer 96® Aqueous Non-Radioactive Cell Proliferation Assay (MTS assay, Promega, Madison, WI). Conditions for the assay were determined based upon time course and were performed in triplicate using 5,000 cells per well in 100 µL of culture medium. After 2 hours of incubation following reagent addition, absorbance (A490) was measured using a Wallac Victor2 1420 Multilabel Counter (Perkin Elmer, Waltham, MA). Viability was expressed as the average A490 of triplicate wells of transfected cells relative to untreated parental cells.

Xenogen Bioluminescent Imaging

Prior to imaging, 600µg of D-luciferin potassium salt (Caliper Life Sciences, Hopkinton, MA) were added to the cell cultures in 20µL of PBS. Samples were placed in a light-tight, low background imaging chamber and a 25 mm (1.0 inch) square back-thinned, back-illuminated, cryogenically-cooled CCD IVIS 100 Imaging System (Xenogen, Alameda, CA) was used to detect photon emission from cells with exposure times ranging from 1 second to 5 minutes. Analyses of the images were performed using Living Image® software (Xenogen) by drawing regions of interest over the plating region and obtaining average radiance values in photons per second per cm^2 per steradian ($p/s/cm^2/sr$) or total flux as photons per second (p/s).

ONE-Glo™ Luciferase Assay

Luciferase expression in mammalian cells was determined using the ONE-Glo™ Luciferase Assay System (Promega, Madison, WI). A stock solution of the commercial reagent was prepared by dissolving the lyophilized powder in the Luciferase Assay Buffer and stored at -20°C. Per vendor protocol, cells were treated with room temperature reagent to minimize adverse effects. Conditions for the assay were performed in triplicate using 5,000 cells per well (96-well format) in 100 µL of culture medium. The light reaction was initiated by adding 100 µL ONE-Glo™ Luciferase reagent to wells. Bioluminescence was measured 10-15 minutes following reagent addition, using a Wallac Victor2 1420 Multilabel Counter (Perkin Elmer, Waltham, MA). Luminescence is expressed as relative to parental control and was normalized to complete medium with reagent.

Validation of Cell Lines

(Data provided by J. Modiano, T. O'Brien, B. Lindborg, A. Franz, R. McElmurray, M. Lewellen)

Animal experiments were carried out according to a protocol approved by the University of Minnesota's Institutional Animal Care and Use Committee (IACUC). Female C57BL/6J mice were purchased from Jackson Laboratories (Bar Harbor, ME) and were 6-8 weeks of age prior to inoculations. Mice were shaved prior to inoculations in the rear left flank. In group 1, control mice received subcutaneous (s.c) inoculations of $5x10^5$ tomato red-tagged, non-

luminescent, mesenchymal stem cells (MSC-tdT) resuspended in 100 µl PBS. In group 2, experimental mice received s.c. inoculations of 5.0 x 10^5 LL3_GL-H2 cells resuspended in 100µl PBS. When performing bioluminescent imaging, animals from both groups received intraperitoneal (i.p.) injections of 150 mg/kg D-luciferin. On the day of injection and at weekly intervals thereafter, animals were anesthetized with isofluorane and fLuc emission was quantified using the IVIS 100 Imaging System chamber (Xenogen, Alameda, CA) with exposure times ranging from 1 minute to 5 minutes.

RESULTS

While many studies have shown successful transduction and transfection of cancer cell lines, it is common to do so using only transient expression methods. Moreover, few studies have focused on a dual tag expression vector that can be tracked both *in vitro* and *in vivo*. In particular, B16 melanoma cell lines and Lewis Lung Carcinoma cell lines have been successfully transfected using viral and plasmid vectors [26], but few stable cell lines suitable for imaging both *in vivo* and *in vitro* had been generated and characterized. As such, we sought to replicate experiments using specific vectors that would enable stable integration of the reporter genes, Green Fluorescent Protein (*GFP*) and firefly Luciferase (*fLuc*).

Transfection of Two Tumor Cell Lines: B16 and LLC

In an initial study to transduce B16 melanoma cells with stable viral vectors, specifically a lentivirus with a GFP cargo, the results indicated low success rate as determined by fluorescence microscopy and flow cytometry (data not shown). To determine if this shortcoming could be resolved using a second plasmid, pKT2PGK-Bsd:GFP_CLP-Luc, trials were conducted to utilize electroporation using Lonza Nucleofection per vendor protocols. While control cells (HEK293) showed relatively high levels (>80%) of GFP expression (Figures 2A & B, Figure 3A & B), there was minimal to no GFP expression visible in B16 and LLC cells respectively (Figures 2C & D, Figure 3C). LLC transfected with positive control

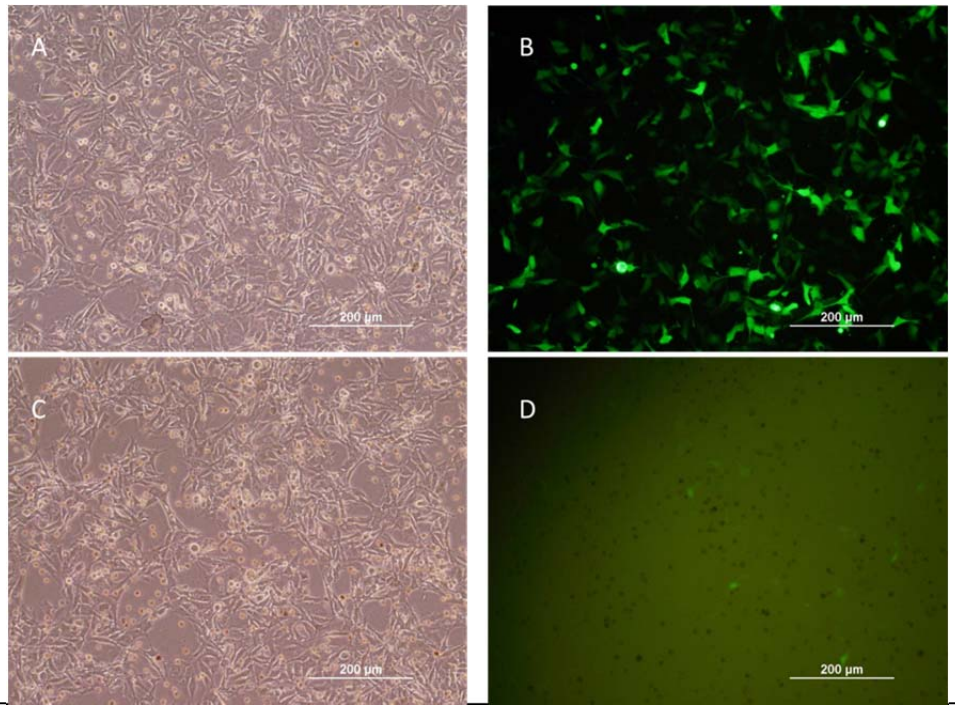

Figure 2. B16 transfection efficiency with Plasmid 1, 24h post transfection. A) Phase contrast with control plasmid. B) Fluorescent with control plasmid. C) Phase contrast with plasmid. D) Fluorescent with plasmid.

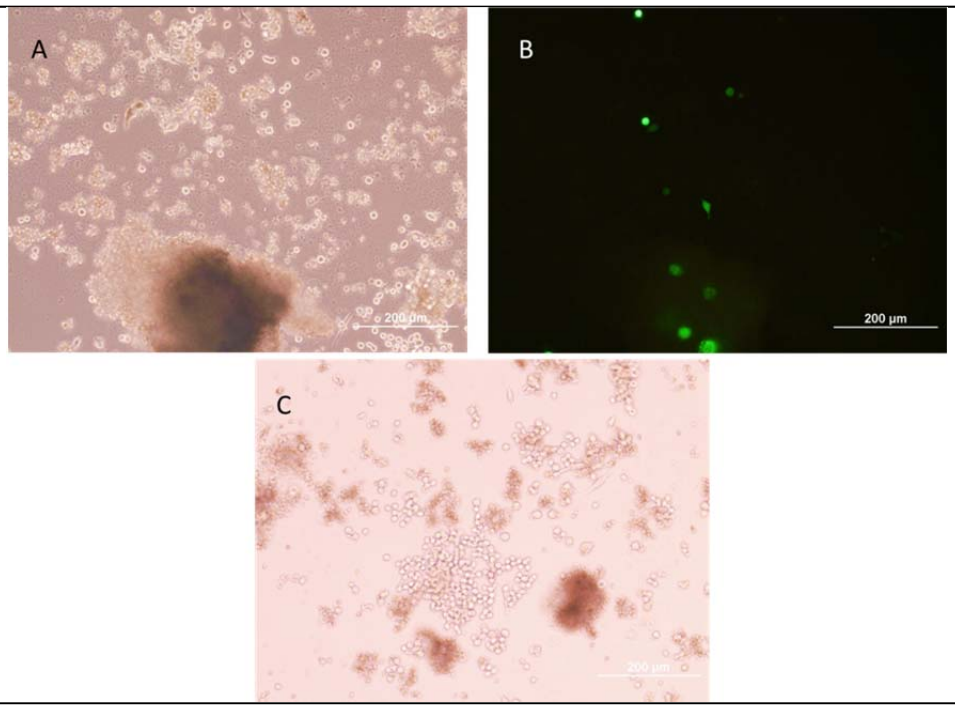

Figure 3. LLC transfection efficiency with Plasmid 1, 24h post transfection. A) Phase contrast with control plasmid. B) Fluorescent with control plasmid. C) Phase contrast with plasmid.

vector also showed high levels of cellular still developed death, suggesting the cells were apoptotically sensitive to this method of transfection. While only a few cells remained, LLC cultures were still repeatedly passaged to confluence and selected using the plasmid antibiotic resistance marker Zeocin.

Following drug selection, detection of fluorescence was monitored by fluorescence microscopy. While LLC_GL cells showed little to no visible GFP expression, B16_GL GFP expression appeared robust (Figure 4A). These results were quantified using flow cytometry. The B16 transfection showed a unimodal shift in GFP expression, suggesting a near uniform population (Figure 4B). The LLC_GL cells, however, showed a multimodal range of GFP expression indicating both GFP positive (59.1%) and GFP negative cells within the population (Figure 4C). These data are consistent with varied genome insertion points within the cell population but do not explain the low visibility via microscopy.

Following confirmation of GFP expression, the expression of fLuc protein was assessed using an *in vivo* luminescent imaging system (Xenogen IVIS) as a surrogate for protein quantification (Figure 5). Intriguingly, the LLC_GL cells showed relatively low levels of luminescence, while the B16 cells showed negligible fLuc expression. There are a number of possibilities which may account for such data, including the potential for the gene expression to be suppressed within these cells [27].

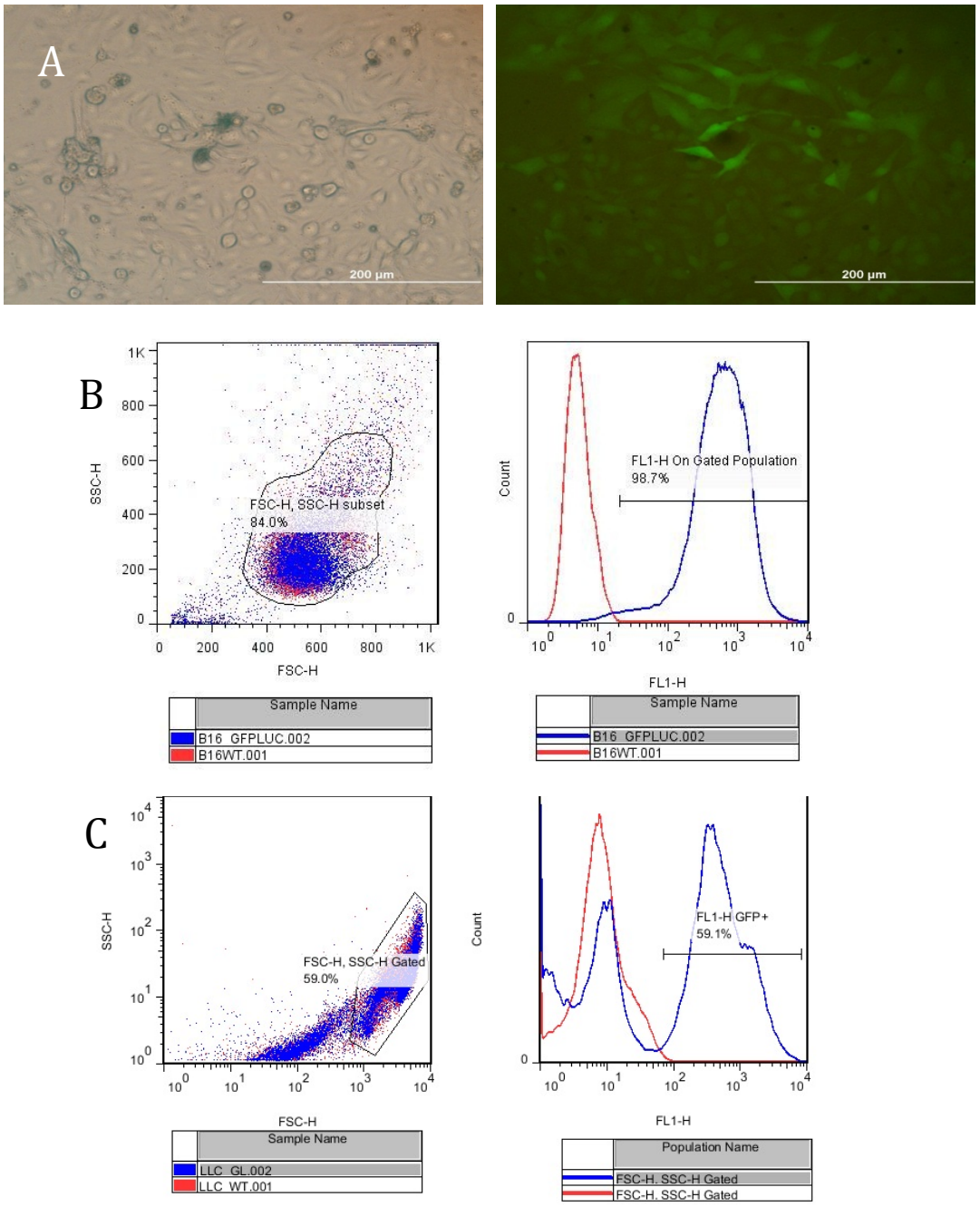

Figure 4. Transfected Tumor Cells Express GFP. A) B16-GL day 10 post-transfection, selected with Zeocin. Left: Phase contrast image. Right: Fluorescent GFP image. B) Flow Cytometry, B16-GL day 10 post-transfection, selected with Zeocin. Cells were gated (Left) to non-transfected B16 parental line control (Red) and compared to transfected B16_GL (Blue). Histogram (Right) shows 98.7% of population expressing GFP. C) Flow Cytometry, LLC_GL post-transfection, selected with blasticidin. Comparisons made between whole population of LLC parental line control (Red) and transfected LLC_GL (Blue). Histogram (Right) indicates 59.1% of LLC_GLs expressing GFP.

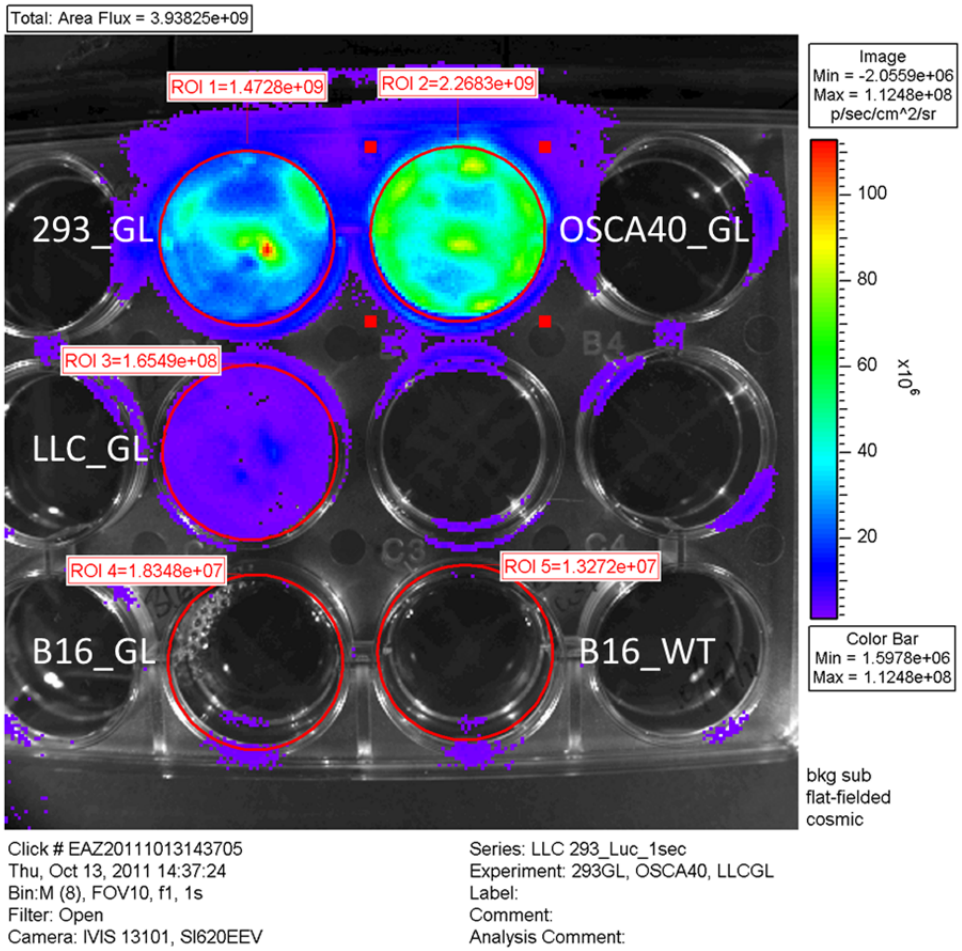

Figure 5. Xenogen *in vitro* Luciferase Imaging for firefly-luciferase expression. 50,000 cells plated, exposure time 1 second. Clockwise: 293_GL positive control, OSCA40_GL positive control, B16 negative control; B16 transfected with Plasmid 1, LLC transfected with Plasmid 1.

Isolation and Clonal Development of LLC_GL

As the transfection process naturally leads to inconsistent integration of the target vectors into the host genome, polyclonal populations of LLC_GLs were expected. Transfected LLC_GL cells were therefore separated based on GFP expression, using FACS (data not shown). This was not only important in narrowing the population for the purposes of monoclonal development, but also in verifying GFP expression. Though labeled GFP^{HI}, the population was selected from the most moderate range of GFP fluorescence, as determined by MFI. This was vital as this population was likely to have sufficiently expressed reporter proteins for visualization, while simultaneously minimizing risk of change to inherent cellular properties [24, 25, 28].

Following sorting, it was important to develop the transfected heterogeneous population, LLC_GL:HI into a monoclonal population via limiting dilution. Doing so establishes more consistent research by eliminating factors associated with having a mixed population: variable reporter expression, growth rate-dependent population shifts, and variable cell behaviors. LLC_GL:HI cells were dissociated and plated (96 well format) at low density (approximately 0.5 cells/well) for isolation purposes. Two populations (LLC_GL:HI1, LLC_GL:HI2) were then chosen for their monoclonal potential and their ability to express GFP. These were expanded for characterization and comparison to parental lineage.

Characterization of LLC_GL Isolated Populations

Isolated populations of GL positive LLC cells (LLC_GL:HI1 and LLC_GL:HI2) were assessed for expression of fLuc using a ONE-Glo™ Luciferase Assay system (Figure 6). Efficient *in vitro* fLuc expression was detected within 10 minutes of the reagent administration. The results indicated that both populations were expressing fLuc at significant levels compared to negative controls, though LLC_GL:HI2 may have a marginally higher level than LLC_GL:HI1. Moreover, as the readout of luminescence within each population approximately doubles with the doubling of cells, these data suggest that fLuc expression is consistent, quantifiable, and correlates to cell number.

Each isolated population was also subjected to FISH staining to determine true clonality and to quantify number of vector insertions with the host genome (Figure 7). Cells imaged during metaphase stage of mitosis indicated that the LLC_GL:HI1 population was not monoclonal (Figure 7 A&B). The data showed at least two derivative lines with distinct chromosomal insertions sites, indicating the population was oligoclonal, or at least biclonal. The second population, LLC_GL:HI2, showed consistent chromosomal insertion sites, at least in approximately the same locations in similarly sized chromosomes (Figure 7C). However, the cell population was not specifically karyotyped to confirm monoclonality.

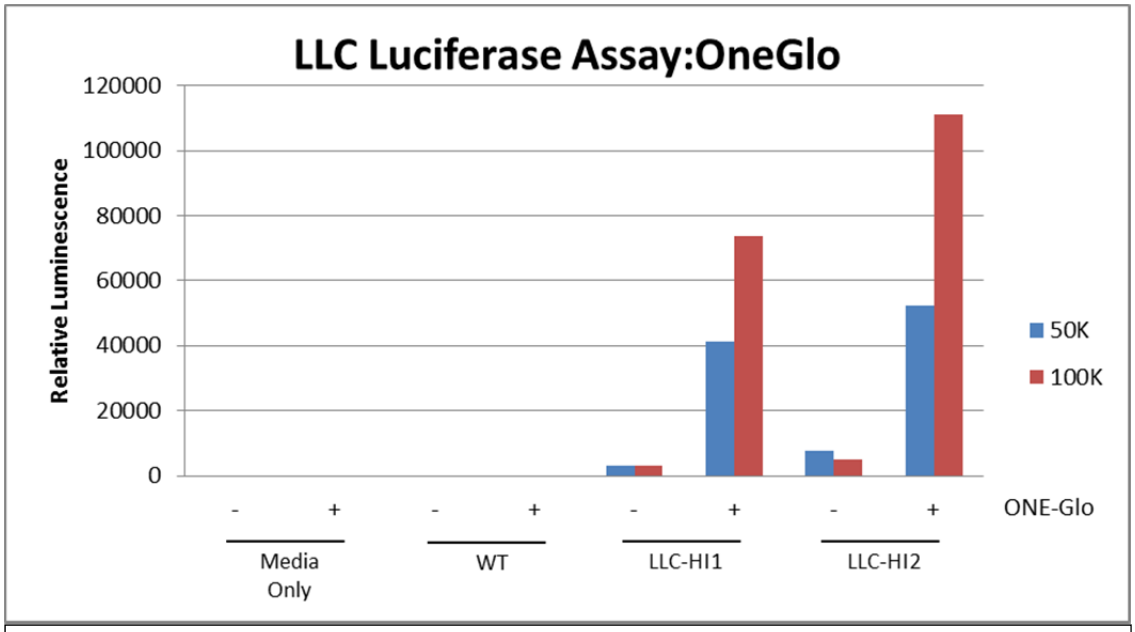

Figure 6. LLC_GL, HI-1 and HI-2, clonal populations express firefly luciferase. Cells assayed after drug and isolation selection.

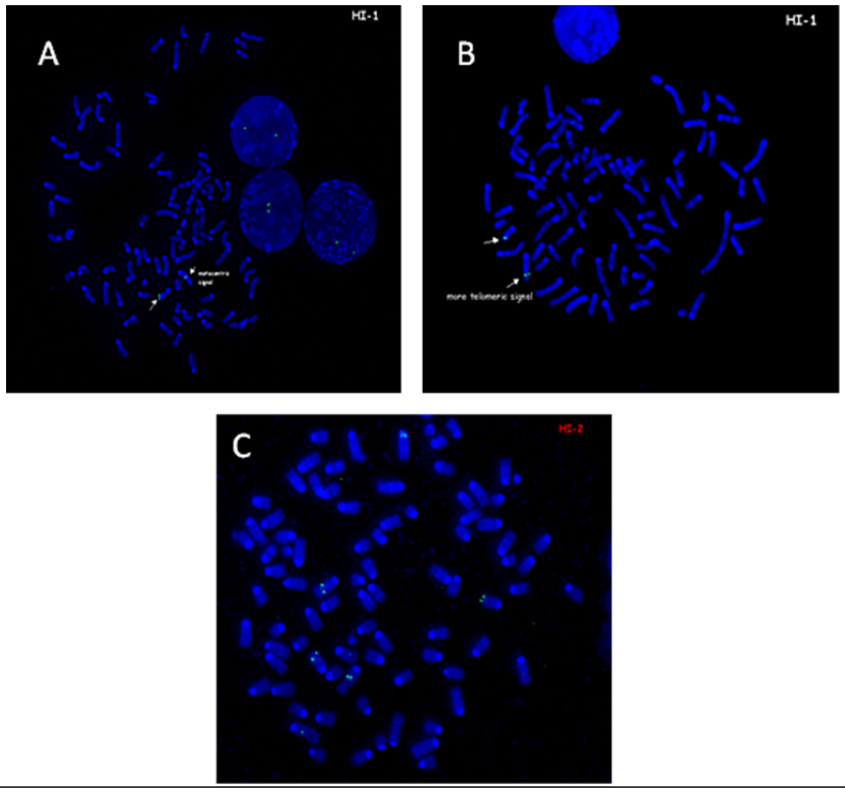

Figure 7. FISH Stain on two sorted, clonal LLC_GL populations. A & B) LLC_GL:HI1 indicates a oliogoclonal population. B) LLC_GL:HI2 indicates a monoclonal population.

Transfection of B16 with Alternative Plasmid

As mentioned above, transfected B16 expression of both GFP and fLuc met with limited success. While it was possible to troubleshoot the process and determine the point of failure for B16 expression of the dual vector, steps were instead taken to optimize vendor protocol for these specific cells (data not shown) and transfect B16 with another plasmid vector. Positive control plasmid (pMax-GFP) transfection indicated >80% efficiency (Figure 8). While the GFP/fLuc plasmid evidenced little GFP via fluorescent microscopy, the transfected population was subjected to drug selection during expansion. Following expansion, GFP expression was visually confirmed via fluorescent microscopy.

Functional assessment of fLuc expression in newly transfected B16 cells was again conducted using Xenogen IVIS system (Figure 9). Results indicated only a half log difference in activity when compared to the untransfected control. This imaging data suggested that the population, though expanded using drug resistance selection, expressed only marginal quantities of fLuc. To confirm this using an alternate assay, fLuc expression within the B16_GL population was quantified using the ONE-Glo™ Luciferase Assay system using cell lysates (data not shown). These data showed robust fLuc activity with the transfected population having a 50 fold difference when compared to wild type. *In vitro* fLuc expression was detected within 5 minutes of the reagent administration.

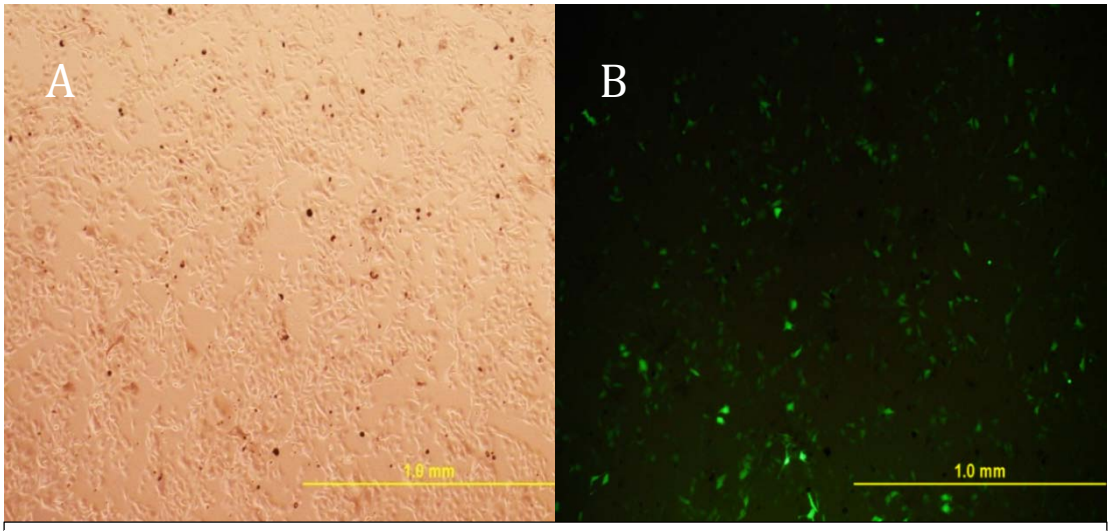

Figure 8. B16 post transfection with control plasmid pMax-GFP.

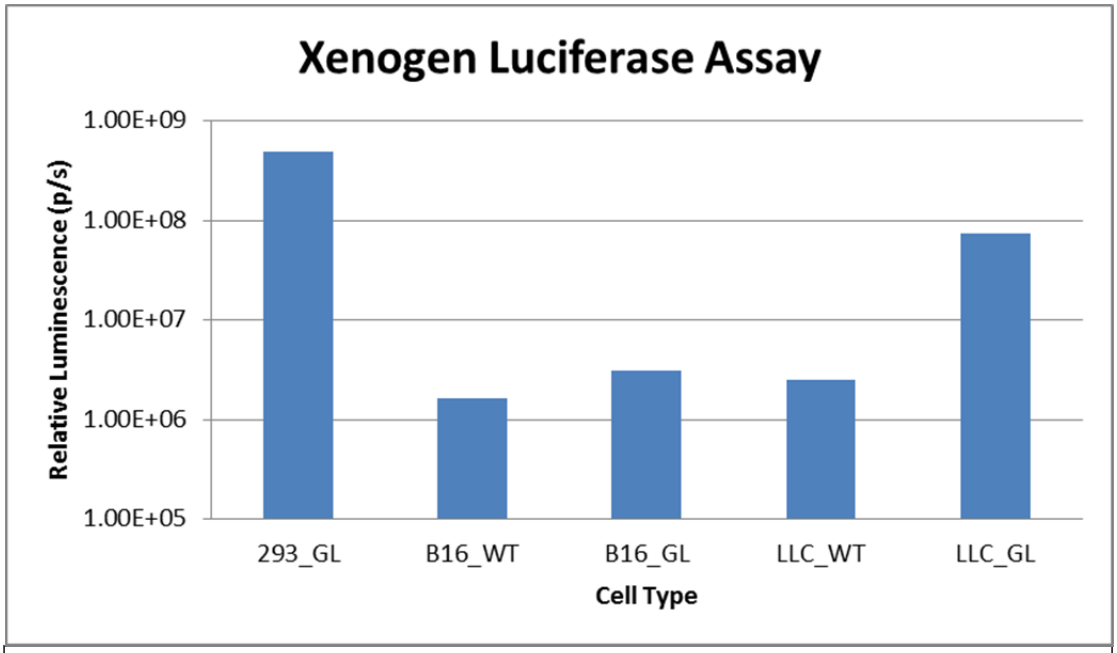

Figure 9. Xenogen Luciferase Imaging for firefly-luciferase expression. 100,000 cells plated per well, exposure time 30 seconds. Left to Right: 293_GL positive control, B16 untransfected (B16_WT) control, B16 transfected with Plasmid 2, LLC untransfected (LLC_WT) control, LLC transfected with Plasmid 1.

Clonal Development and Characterization of B16_GL Isolated Populations

Following determination that at least a portion of the B16_GL cells were expressing fLuc or GFP proteins, cells were sorted into two populations using FACS (data not shown). Similar to the previous sorting schema, B16_GL:HI cells were selected from the most moderate range of GFP fluorescence, as determined by MFI. Following sorting, fLuc activity was confirmed (Figure 10). A second population, B16_GL:LO, was selected based on being specifically dimmer and distinct from the B16_GL:HI population. Based on a qualitative cell growth assay showing growth rates approximate to the parental lineage, further experiments were limited to use of B16_GL:LO1. Those cells were dissociated and plated using limiting dilution techniques. Two populations were chosen based on their monoclonal potential and GFP confirmation, expanded and passaged for further analysis.

Similar to that of the transfected LLC cells, B16_GL:LO1 were assessed for expression of fLuc using the ONE-Glo Luciferase Assay system (Figure 11). Efficient *in vitro* fLuc expression was detected within 10 minutes of the reagent administration. The data indicated that the population was expressing fLuc at markedly higher levels compared to controls.

The growth curve of the isolated population of transfected B16 cells was compared to that of the parental lineage (Figure 12). In this experiment, cells

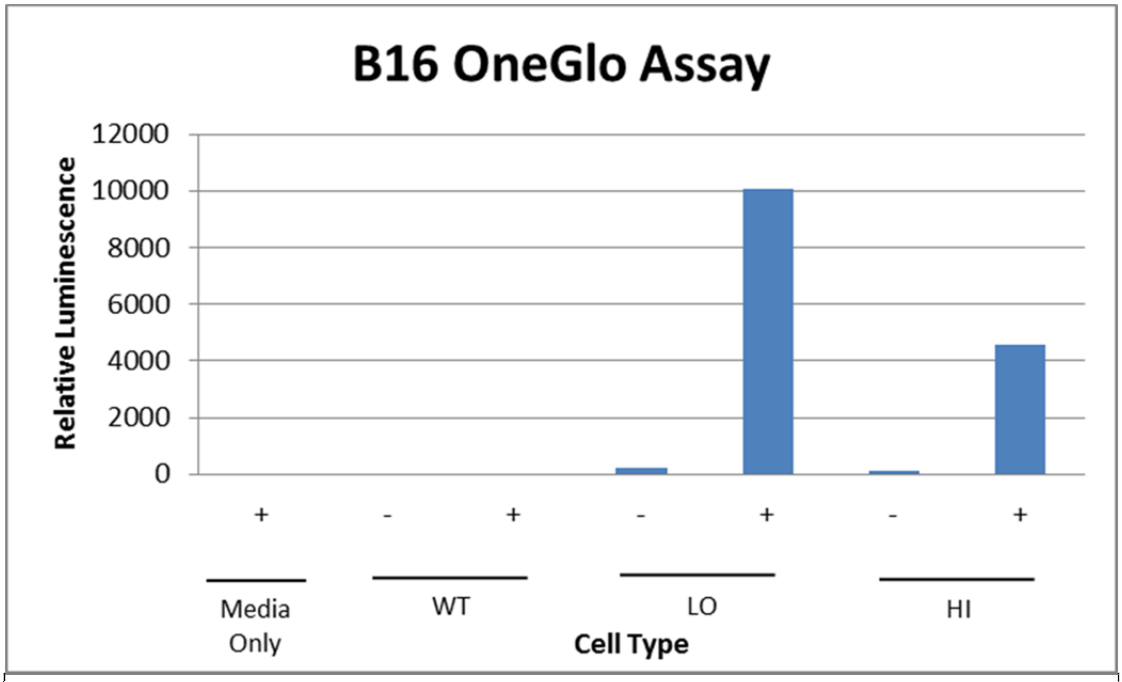

Figure 10. OneGlo *In Vitro* Luciferase Imaging for firefly-luciferase expression in sorted B16_GL cell lines. Cell density plated at $.5x10^5$ respectively.

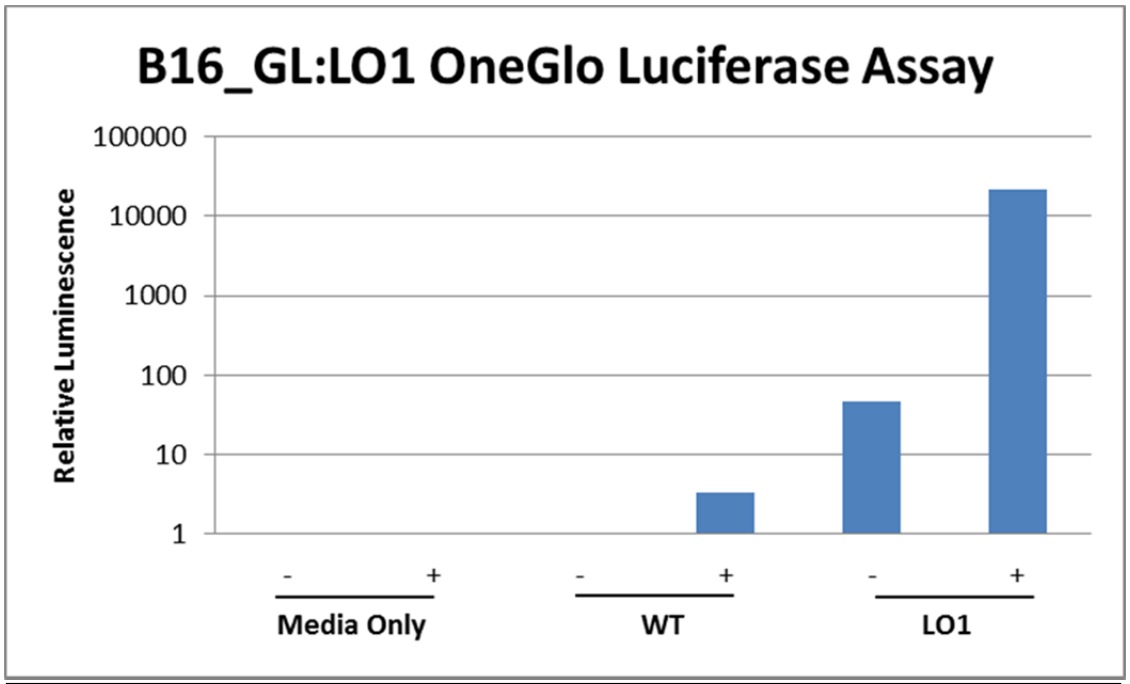

Figure 11. OneGlo *In Vitro* Luciferase Imaging for firefly-luciferase expression in limiting dilution clone selection. Cell density plated at $.5x10^5$ respectively.

were plated at a density of 5000 cells per well in a 96-well plate. Measurements were taken at 24h, 48, and 72h post plating. By the 48 hour time point, the transfected B16 cells expanded to a point where maximum growth rate was curbed due to plate confluence. Regardless, these data suggest that the insertion of the dual vector might have enhanced the vigor and aggressiveness of the parental lineage's rate of growth by approximately two fold.

Validation of Cell Lines In Vivo and In Vitro

To assess functionality of the dual labeled tumor cells both in vivo and in vitro, groups of mice were inoculated in their rear left flanks with either labeled MSC-tdT cells or the LLC_GL:HI2 cells. After seven days post injection, the mice were examined for fLuc associated bioluminescence using the Xenogen IVIS. Control mice inoculated with PBS (data not shown), or MSC-tdT lacking a bioluminescent marker, presented no visible flank tumor and negligible luminescent signal (Figure 13A). The data remained consistent at future time points and when extending imaging time increments. As shown in Figure 13B, light emission as detected by the imaging system correlated to site of injection. Over time, bioluminescent signal correlated with tumor burden (data not shown). After resection, tumors were fixed and imaged with confocal microscopy (Figure 14). Data shows that GFP-postive LLC_GL:HI2 tumor cells (Green) and control MSC-tdT (Red) localizing adjacent to each other, providing

evidence that gene suppression is not problematic, *in vivo* expression is robust and trackable via fluorescent microscopy.

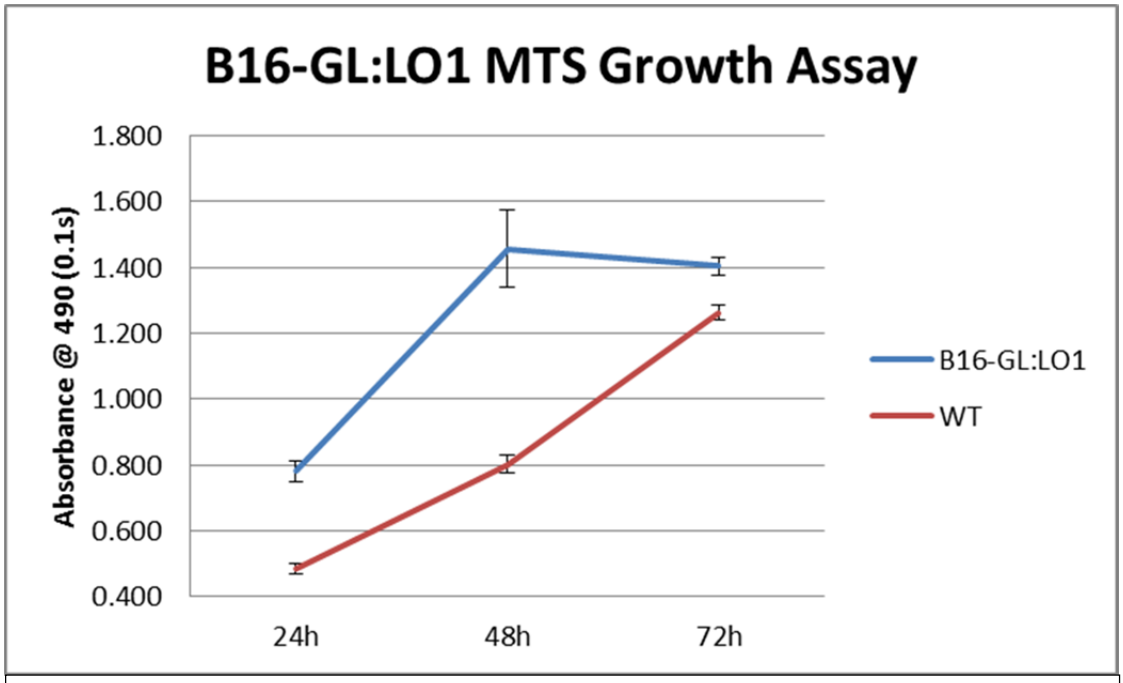

Figure 12. MTS growth assay following clonal selection of transfected B16 cells.

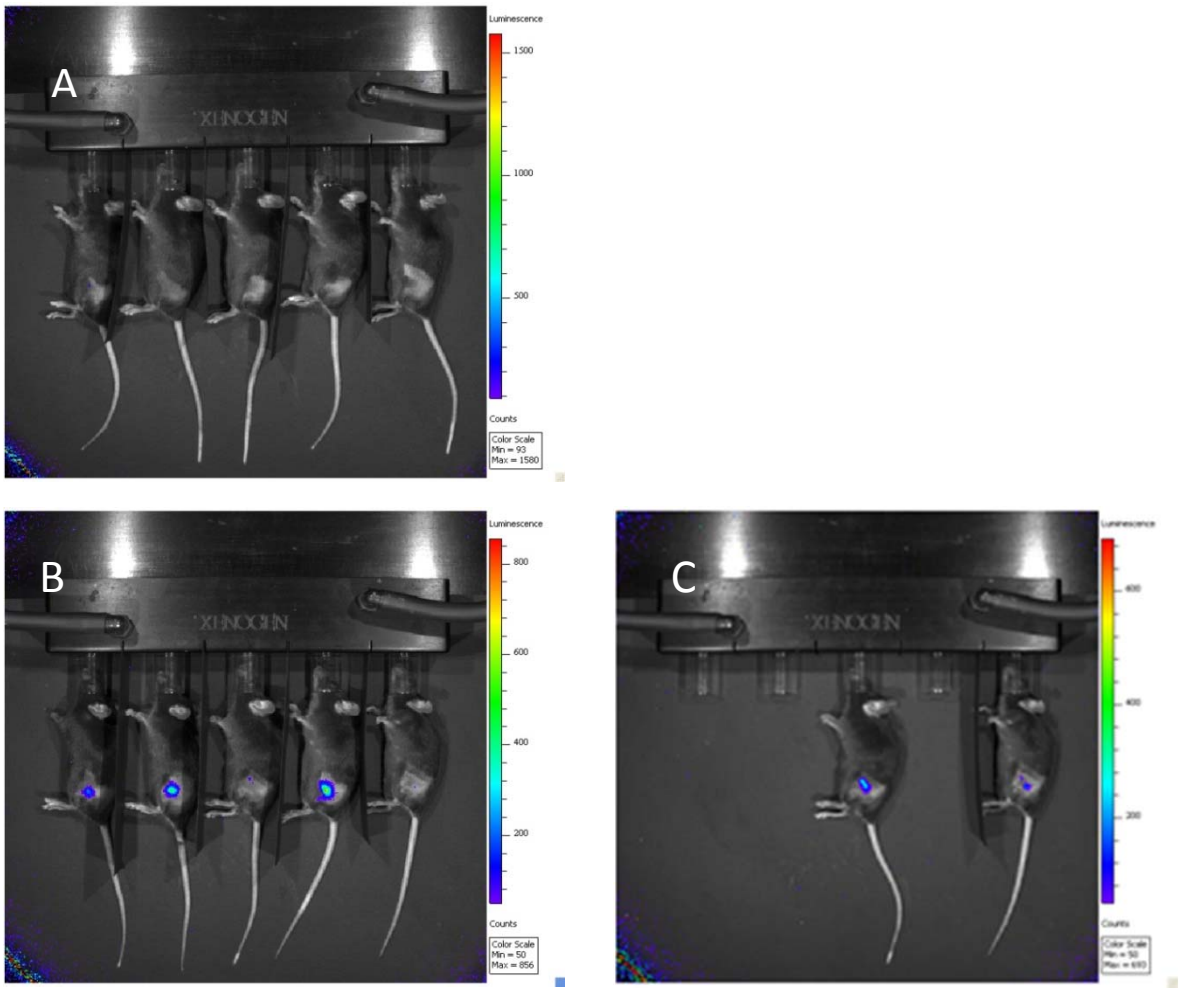

Figure 13. Xenogen *In Vivo* tumorigenicity assay of LLC_GL:HI2. A) Mice inoculated with non-labeled MSC-tdTs; negative control. B) Mice inoculated with LLC_GL:HI2 and imaged for 1 minute. C) Mice inoculated with LLC_GL:HI2 and imaged for 5 minutes (Data provided by J. Modiano, M. Lewellen, R. McElmurray, B. Lindborg, A. Franz).

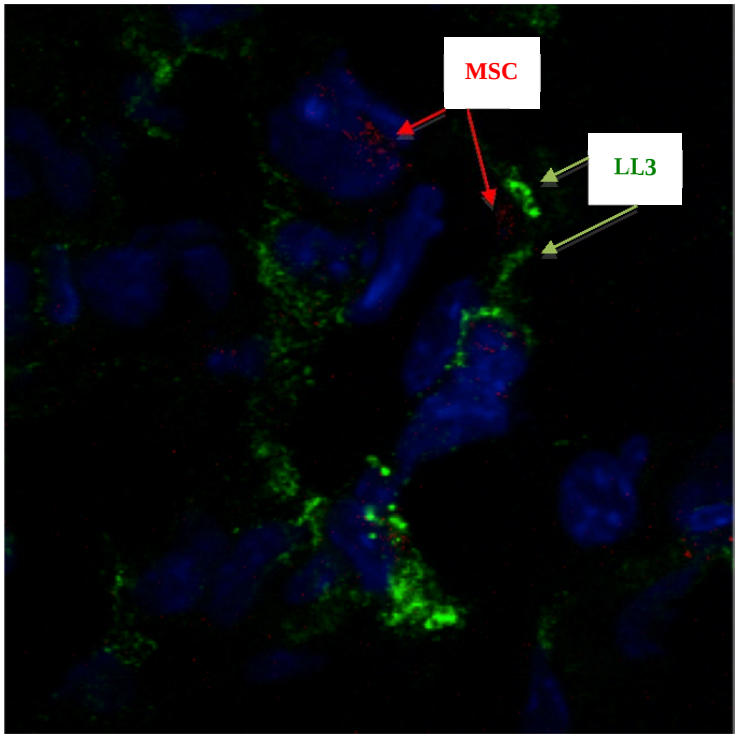

Figure 14. Fluorescent Confocal Microscopy of *In Vitro* LLC_GL:HI2 Tumor. Green= LLC_GL:HI2, Red=MSC-tDT; Blue=DAPI staining. (Data provided by T. O'Brien)

DISCUSSION

Although understanding of cancer as a whole increases each year, the ability to translate this knowledge into successful application and treatment has met with limited success [29, 30]. In order to provide more relevant therapies for cancer, tumor modeling must play a critical role. One criticism regarding current modeling is that there are few which permit a facile way of assessing tumor progression or response to trial therapies. Current imaging modalities include magnetic resonance imaging (MRI), micro-positron emission topography (PET), and micro-computed tomography (CT). While each of these offers a high resolution, three dimensional imaging of tumor structure, they are relatively expensive, resource prohibitive and require complex data analysis [31, 32]. Alternatively, bioluminescent imaging models are highly accurate, relatively inexpensive, require only short collection times, don't require animal sacrifice, and multiple subjects can be assayed simultaneously. As such, this technology has become a useful tool for quantifying tumor burden *in vivo*, with fewer animals, and in real time [26, 33]. However, its mechanism of action is dependent upon ATP and thus only live cells can be imaged. This drawback is not present in models using fluorescent proteins, such as GFP. Fluorescence imaging can be done at different resolutions and depth penetrations, and is dependent upon energy from an external source of light, not a chemiluminescent reaction. The models which are put forth in this research were designed to leverage these two established models, bioluminescent and fluorescent imaging. The results, though preliminary at this point, set the stage

for an immunologically replete murine tumor system with which we can image and track tumors, both *in vivo* and *in vitro,* using dual reporter proteins.

In our research efforts to transfect our cell lines, we found that B16 melanoma may be resistant to lentiviral transduction (data not shown) as determined by GFP expression. This contradicts with others that have shown success with similar attempts [34]. However, to simplify the approach and reduce potential toxicity in application, we pursued an approach using a proven electroporation system. Initial trials resulted in unexpectedly high levels of cell death but may have been due to improperly defined experimental conditions. Though multiple conditions were examined for higher efficiency, immediately prior to the implementation the previously transfected cells successfully expanded and were used. It should, however, be cautioned that this process may have selected for more vigorous or aggressive tumor cells. This possibility will require testing using both *in vitro* and *in vivo* growth assessments.

The transfected cell lines, B16_GL and LLC_GL, were tested for GFP and fLuc expression. Interestingly, the robustly expanding B16 population had negligible expression of fLuc as measured by Xenogen total flux (p/s). In a study by Zhu et al., it was discovered that over time, it was possible for transgenes to be silence via CpG methylation [35]. This led us to consider the possibility that our own fLuc transgene was being repressed as well. Thus the cell line was discarded. In retrospect, this was likely a misinterpretation of the data. In the trials using an alternative plasmid (Figure 1), B16 showed robust GFP expression as determined by both flow cytometry and fluorescent

microscopy. When a lysis-mediated assay (ONE-Glo™ Luciferase Assay System) was used to quantify fLuc activity, it indicated substantial expression. Data regarding the Xenogen IVIS system was re-examined and it was determined that average radiance (p/s/cm^2/str), rather than total flux (p/s), corroborated the findings. This metric agrees with standards used regarding fLuc labeled mice [26].

In each of our stably transfected cell lines, flow cytometry data supported the predicted possibility of a heterogeneous population which opened the potential for criticism of non-uniform cellular behavior. Thus, it was critical to sort the respective populations and perform limiting tissue culture dilutions to establish monoclonal cultures. As there were no indications of altered growth rates or morphological disparities in the sorted GFP^{HI} LLC_GLs, limiting dilutions were selected from these cultures. However, culturing of GFP^{HI} B16_GL cells required more frequent passaging when compared to GFP^{LO} or the parental lines. As such limiting dilution was performed on GFP^{LO} B16_GLs. Though alternative isolation techniques such as FACS-based isolation may result in higher degrees of efficiency, this approach is the current standard for forming homogeneous populations.

Following clonal development, populations were again tested for reporter gene expression and characterizations were initiated. These assays included confirmation of expression of the dual reporter genes, growth rate comparisons to parental lines, and FISH staining for consistent chromosomal insertion sites. This data indicated that at least one population, LLC_GL/HI2, was likely

monoclonal. However, isolated colonies of transfected B16 cells should at least be subjected to similar assessments. For further confirmation, and for quantification of gene insertion, all cell lines should be subjected to clonal determination using karyotyping or molecular PCR analysis [36].

While each of the isolated cell populations requires additional analysis regarding growth comparisons, metastatic potential, *in vivo* tumorigenesis, and validation of cell lineage to name a few examples, there are some indications that the novel cell lines may be useful in future tumor burden assays. In particular, when experiments were performed to examine the growth potential tumorgenicty and *in vivo* tracking capacity, the LLC-HI2 population showed robust fLuc signaling *in vivo*. This was in addition to the GFP signaling confirmed in tumors removed and analyzed *in vitro* post mortem. Together, these provide proof of concept that this dual reporter system is functional and may lead to improved modeling.

One particular advantage this model offers in cancer research pertains to the complex roles which inflammation and immune cells play in cancer development. Immune cells, such as T cells, natural killer (NK) cells, B cells, dendritic cells and macrophages each contribute to complex tumor development and progression in a variety of ways [2, 37-40]. As such, it is vital to making progress in cancer therapeutics to understand the intricacies these key components mediate. As a whole, this is quite a challenge and requires animal modeling which is immunologically intact. As our tumor models are syngeneic for the C57BL/6 mouse, and thus do not modify the immune system,

they can be utilized for immune relevant studies. Though reports have indicated the potential for GFP and fLuc to elicit an immune response [23, 24], this potential should be examined in preliminary studies with our cell lines to minimize misinterpretation of tumor studies.

In combination, the data herein shows we were able to stably transfect two tumor cell lines, B16 and Lewis lung carcinoma, with dual reporter plasmid vectors, confirm expression of the reporter genes, provide evidence that they are not suppressed *in vivo* and can be used to track tumor burden. We also demonstrated that the same tumor cells can also be analyzed using *in vitro* fluorescent microscopy following post-mortem resection. Because these models offer advantages over other alternative tumor imaging models, these have potential applicability in future studies regarding non-small lung cell carcinomas and melanomas, specifically as it relates to tumor burden, metastasis, and invasion. In addition, these models have strong potential for application in studies requiring immune replete tumor animals. Furthermore, the approach taken here, in using stably integrated dual reporters, may serve useful in other tumor models in general.

BIBLIOGRAPHY

1. Hanahan, D. and R.A. Weinberg, *The hallmarks of cancer.* Cell, 2000. **100**(1): p. 57-70.
2. Hanahan, D. and R.A. Weinberg, *Hallmarks of cancer: the next generation.* Cell, 2011. **144**(5): p. 646-74.
3. Rangarajan, A. and R.A. Weinberg, *Opinion: Comparative biology of mouse versus human cells: modelling human cancer in mice.* Nat Rev Cancer, 2003. **3**(12): p. 952-9.
4. Lin, T., et al., *Targeted expression of green fluorescent protein/tumor necrosis factor-related apoptosis-inducing ligand fusion protein from human telomerase reverse transcriptase promoter elicits antitumor activity without toxic effects on primary human hepatocytes.* Cancer Res, 2002. **62**(13): p. 3620-5.
5. Aizawa, H., M. Sameshima, and I. Yahara, *A green fluorescent protein-actin fusion protein dominantly inhibits cytokinesis, cell spreading, and locomotion in Dictyostelium.* Cell Struct Funct, 1997. **22**(3): p. 335-45.
6. Nalaskowski, M.M., et al., *A toolkit for graded expression of green fluorescent protein fusion proteins in mammalian cells.* Anal Biochem, 2012. **428**(1): p. 24-27.
7. Chatterjee, R., *Cell biology. Cases of mistaken identity.* Science, 2007. **315**(5814): p. 928-31.
8. *UKCCCR guidelines for the use of cell lines in cancer research.* Br J Cancer, 2000. **82**(9): p. 1495-509.
9. MacLeod, R.A., et al., *Widespread intraspecies cross-contamination of human tumor cell lines arising at source.* Int J Cancer, 1999. **83**(4): p. 555-63.
10. Colgin, L.M. and R.R. Reddel, *Telomere maintenance mechanisms and cellular immortalization.* Curr Opin Genet Dev, 1999. **9**(1): p. 97-103.
11. Frese, K.K. and D.A. Tuveson, *Maximizing mouse cancer models.* Nat Rev Cancer, 2007. **7**(9): p. 645-58.
12. Waterston, R.H., et al., *Initial sequencing and comparative analysis of the mouse genome.* Nature, 2002. **420**(6915): p. 520-62.
13. Sharkey, F.E. and J. Fogh, *Considerations in the use of nude mice for cancer research.* Cancer Metastasis Rev, 1984. **3**(4): p. 341-60.
14. Price, J.E., et al., *Tumorigenicity and metastasis of human breast carcinoma cell lines in nude mice.* Cancer Res, 1990. **50**(3): p. 717-21.
15. Hanna, N., T.W. Davis, and I.J. Fidler, *Environmental and genetic factors determine the level of NK activity of nude mice and affect their suitability as models for experimental metastasis.* Int J Cancer, 1982. **30**(3): p. 371-6.
16. Gordon, J.W., et al., *Genetic transformation of mouse embryos by microinjection of purified DNA.* Proc Natl Acad Sci U S A, 1980. **77**(12): p. 7380-4.
17. Singer, O. and I.M. Verma, *Applications of lentiviral vectors for shRNA delivery and transgenesis.* Curr Gene Ther, 2008. **8**(6): p. 483-8.
18. Gama Sosa, M.A., R. De Gasperi, and G.A. Elder, *Animal transgenesis: an overview.* Brain Struct Funct, 2010. **214**(2-3): p. 91-109.

19. Sharpless, N.E. and R.A. Depinho, *The mighty mouse: genetically engineered mouse models in cancer drug development.* Nat Rev Drug Discov, 2006. **5**(9): p. 741-54.
20. Hassan, M., et al., *Fluorescence lifetime imaging system for in vivo studies.* Mol Imaging, 2007. **6**(4): p. 229-36.
21. Ivics, Z., et al., *Molecular reconstruction of Sleeping Beauty, a Tc1-like transposon from fish, and its transposition in human cells.* Cell, 1997. **91**(4): p. 501-10.
22. Izsvak, Z., et al., *Efficient stable gene transfer into human cells by the Sleeping Beauty transposon vectors.* Methods, 2009. **49**(3): p. 287-97.
23. Stripecke, R., et al., *Immune response to green fluorescent protein: implications for gene therapy.* Gene Ther, 1999. **6**(7): p. 1305-12.
24. Jeon, Y.H., et al., *Immune response to firefly luciferase as a naked DNA.* Cancer Biol Ther, 2007. **6**(5): p. 781-6.
25. Dass, C.R. and P.F. Choong, *GFP expression alters osteosarcoma cell biology.* DNA Cell Biol, 2007. **26**(8): p. 599-601.
26. Craft, N., et al., *Bioluminescent imaging of melanoma in live mice.* J Invest Dermatol, 2005. **125**(1): p. 159-65.
27. Garrison, B.S., et al., *Postintegrative gene silencing within the Sleeping Beauty transposition system.* Mol Cell Biol, 2007. **27**(24): p. 8824-33.
28. Agbulut, O., et al., *GFP expression in muscle cells impairs actin-myosin interactions: implications for cell therapy.* Nat Methods, 2006. **3**(5): p. 331.
29. Suggitt, M. and M.C. Bibby, *50 years of preclinical anticancer drug screening: empirical to target-driven approaches.* Clin Cancer Res, 2005. **11**(3): p. 971-81.
30. Hackam, D.G. and D.A. Redelmeier, *Translation of research evidence from animals to humans.* JAMA, 2006. **296**(14): p. 1731-2.
31. Hollingshead, M.G., et al., *A potential role for imaging technology in anticancer efficacy evaluations.* Eur J Cancer, 2004. **40**(6): p. 890-8.
32. Hong, H., et al., *Non-invasive cell tracking in cancer and cancer therapy.* Curr Top Med Chem, 2010. **10**(12): p. 1237-48.
33. Weissleder, R. and V. Ntziachristos, *Shedding light onto live molecular targets.* Nat Med, 2003. **9**(1): p. 123-8.
34. Ray, P., et al., *Imaging tri-fusion multimodality reporter gene expression in living subjects.* Cancer Res, 2004. **64**(4): p. 1323-30.
35. Zhu, J., et al., *High-level genomic integration, epigenetic changes, and expression of sleeping beauty transgene.* Biochemistry, 2010. **49**(7): p. 1507-21.
36. Yamamoto, N., et al., *Determination of clonality of metastasis by cell-specific color-coded fluorescent-protein imaging.* Cancer Res, 2003. **63**(22): p. 7785-90.
37. Qian, B.Z. and J.W. Pollard, *Macrophage diversity enhances tumor progression and metastasis.* Cell, 2010. **141**(1): p. 39-51.
38. Du, G., et al., *Human IL18-IL2 fusion protein as a potential antitumor reagent by enhancing NK cell cytotoxicity and IFN-gamma production.* J Cancer Res Clin Oncol, 2012.

39. Mizukami, S., et al., *Differential MyD88/IRAK4 requirements for cross-priming and tumor rejection induced by heat shock protein 70-model antigen fusion protein.* Cancer Sci, 2012. **103**(5): p. 851-9.
40. Lucas, P.J., et al., *Transforming growth factor-beta pathway serves as a primary tumor suppressor in CD8+ T cell tumorigenesis.* Cancer Res, 2004. **64**(18): p. 6524-9.